ISSN 1070-3632, Russian Journal of General Chemistry, 2014, Vol. 84, No. 8, pp. 1463–1467. © Pleiades Publishing, Ltd., 2014.
Original Russian Text © O.A. Vorontsova, O.E. Lebedeva, 2014, published in Zhurnal Obshchei Khimii, 2014, Vol. 84, No. 8, pp. 1233–1238.

Mg–Al–Fe-Containing Layered Hydroxides

O. A. Vorontsova and O. E. Lebedeva

Belgorod State National Research University, ul. Pobedy 85, Belgorod, 308015 Russia
e-mail: vorontsova@bsu.edu.ru

Received January 9, 2014

Abstract—Magnesium–aluminum–iron layered hydroxides with hydrotalcite-like structure have been synthesized, and their chemical composition and crystal lattice parameters have been elucidated. Thermal decomposition of the iron-containing layered hydroxides has been studied by X-ray diffraction, thermogravimetry, and IR spectroscopy; the decomposition starts with loss of interlayer water, followed by dehydroxylation of metal hydroxide layers and decomposition of anions at higher temperature. Onset of the both decomposition stages has been shifted to lower temperature with increasing iron fraction in the sample. Magnesium–aluminum–iron hydroxides restore their structure after annealing and subsequent rehydration.

Keywords: layered hydroxide, calcination, structure recovery

DOI: 10.1134/S1070363214080015

Layered hydroxides are known as hydrotalcite-like materials or anionic clays. The latter name is associated with their peculiar structure, in particular, with the presence of exchangeable anions in the interlayer space. The ideal formula of these compounds is $M^{2+}_{1-x}M^{3+}_{x}(OH)_2[(A^{n-})_{x/n}\cdot mH_2O]$, M^{2+} being Mg^{2+}, Co^{2+}, Ni^{2+}, Cu^{2+}, or Zn^{2+}; M^{3+} being Al^{3+}, Cr^{3+}, or Fe^{3+}; and An being any anion (CO_3^{2-}, OH^-, NO_3^-, SO_4^{2-}, Cl^-, etc.) [1].

Layered hydroxides are generally described as composed of octahedrons with the metal cation in their centers and six oxygen atoms in the vertices [2–4]; the octahedrons network forms brucite-like layers. The isomorphous substitution of double-charged cations by triple-charged ones results in the appearance of excessive positive charge that is compensated for by anions in the interlayer space.

Due to the specific properties, layered hydroxides are applied as promising precursors of catalysts [5–7], finely dispersed mixed oxides [8], and sorbents [9]. The ability of layered hydroxides to restore their layered structure after cyclic dehydration−rehydration has been discussed in [2, 10, 11].

Preparation and properties of layered hydroxides with complex cation compositions are fairly well documented, but the composition−property and the structure−property correlations have still been scarcely studied on a systematic basis for such compounds. Synthesis of iron-containing layered hydroxides has been mentioned in the only publication [1], but their properties have never been studied and described in detail.

In this work we prepared and studied 8 samples of magnesium–aluminum–iron hydroxides, hereinafter referred to as Mg/AlFe$_x$ (x standing for iron molar fraction with respect to sum of the trivalent cations). For the sake of comparison, we also synthesized hydrotalcite, layered magnesium–aluminum hydroxide (Mg/Al) and two magnesium–iron hydroxides (Mg/Fe and Mg/Fe') differing in the cations ratio.

The X-ray diffraction (XRD) patters of the synthesized samples were typical of layered hydroxides (Fig. 1).

Chemical formulas of the synthesized layered hydroxides and the respective fractions of di- and trivalent cations were determined by elemental analysis and thermogravimetry, and the hydroxides crystal lattice parameters were derived from the XRD data (Table 1).

The structural parameter of layered hydroxides most widely discussed in the literature, c, is calculated as $3d/n$ from the data for the first (strongest) peak in the XRD pattern, corresponding to the (003) plane. This parameter characterizes the interlayer spacing. The crystal lattice parameter a reflects the distance

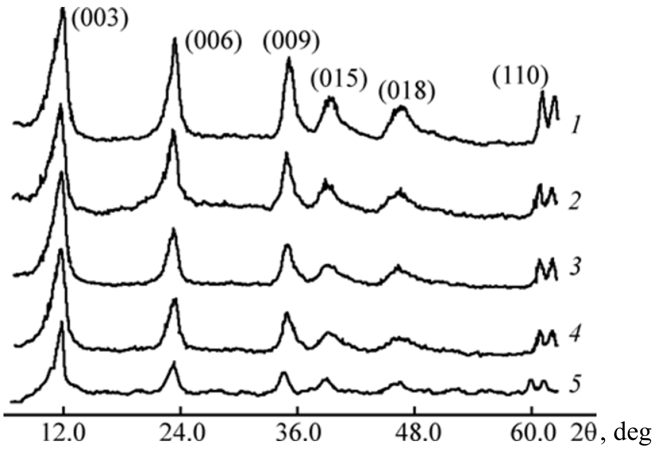

Fig. 1. X-ray diffraction patterns of the layered hydroxides: (*1*) Mg/AlFe$_2$, (*2*) Mg/AlFe$_6$, (*3*) Mg/AlFe$_{10}$, (*4*) Mg/AlFe$_{23}$, and (*5*) Mg/Fe.

between the neighboring cations in the brucite-like layer and is equal to double the interplanar spacing for the (110) plane [12].

As seen from data in Table 1, the *a* parameter tended to increase with increasing fraction of iron. The *c* parameter varied irregularly, apparently being a function of both iron fraction and the ratio of M^{2+} to M^{3+} cations. That was confirmed by different *c* values in the cases of two magnesium–iron hydroxides differing in Mg/Fe ratio.

In this work, we focused at behavior of the layered hydroxides upon heating. The thermal analysis data (Fig. 2) were typical of layered hydroxides.

The TGA curves revealed two stages of the weight loss. The first stage (150–250°C) was assigned to desorption of physically bound water from the interlayer space. The second stage (300–450°C) was associated with partial dehydroxylation of the layers and thermal decomposition of anions (carbonate) in the interlayer space. The DSC curves showed two well-defined endothermic peaks. The first one (220–250°C) was well correlated with the weight loss data and was assigned to the loss of interlayer water. The second minimum was observed at 350–420°C; the temperature corresponded to collapse of the layered structure and formation of the oxides mixture. The first endothermic peak was 20–40% weaker than the second one in the cases of all hydroxides, except for the Mg/Al and Mg/Fe samples.

With increasing iron fraction in the sample, the onsets of the both endothermic effects were shifted towards lower temperature.

IR spectra of the samples at room temperature contained characteristic bands typical of other hydrotalcite-like compounds (Fig. 3). The bands below 900 cm^{-1}, observed in all the IR spectra, were assigned to vibrations of the metal–oxygen and the metal–metal bonds in the brucite-like layer. The fairly broad band at 3460–3550 cm^{-1} was assigned to O–H stretching in the metal hydroxide layers. The well-defined shoulder at 3035–3170 cm^{-1} was associated with O–H stretching in the interlayer water molecules. Very strong and much narrower band at 1360–1385 cm^{-1} was due to

Table 1. Chemical formula and crystal lattice parameters of the studied layered hydroxides

Hydroxide^a	Chemical formula	*c*, Å^b	*a*, b^b	*V*, Å^3	Mg : Me^{III}
Mg/Al	$Mg_{0.70}Al_{0.30}(OH)_2(CO_3)_{0.15}\cdot0.82H_2O$	23.29	3.06	188.9	2.3
Mg/AlFe$_2$	$Mg_{0.67}Al_{0.32}Fe_{0.01}(OH)_2(CO_3)_{0.16}\cdot0.95H_2O$	23.70	3.07	193.4	2.1
Mg/AlFe$_{2-1}$	$Mg_{0.82}Al_{0.17}Fe_{0.01}(OH)_2(CO_3)_{0.09}\cdot0.96H_2O$	23.70	3.07	193.4	4.6
Mg/AlFe$_6$	$Mg_{0.68}Al_{0.30}Fe_{0.02}(OH)_2(CO_3)_{0.16}\cdot0.93H_2O$	23.81	3.07	194.3	2.1
Mg/AlFe$_{10}$	$Mg_{0.68}Al_{0.29}Fe_{0.03}(OH)_2(CO_3)_{0.16}\cdot0.94H_2O$	23.60	3.07	192.6	2.1
Mg/AlFe$_{11}$	$Mg_{0.84}Al_{0.14}Fe_{0.02}(OH)_2(CO_3)_{0.08}\cdot0.88H_2O$	23.70	3.07	193.4	5.2
Mg/AlFe$_{20}$	$Mg_{0.83}Al_{0.14}Fe_{0.03}(OH)_2(CO_3)_{0.09}\cdot0.91H_2O$	23.70	3.07	193.4	4.9
Mg/AlFe$_{23}$	$Mg_{0.73}Al_{0.21}Fe_{0.06}(OH)_2(CO_3)_{0.14}\cdot0.94H_2O$	23.70	3.07	193.4	2.7
Mg/AlFe$_{31}$	$Mg_{0.67}Al_{0.23}Fe_{0.10}(OH)_2(CO_3)_{0.17}\cdot0.93H_2O$	23.60	3.07	192.6	2.0
Mg/Fe	$Mg_{0.67}Fe_{0.33}(OH)_2(CO_3)_{0.17}\cdot0.88H_2O$	23.60	3.11	197.7	2.0
Mg/Fe'	$Mg_{0.75}Fe_{0.25}(OH)_2(CO_3)_{0.13}\cdot0.88H_2O$	23.49	3.11	196.8	3.0

[a] The index at Fe relates to the atomic percent of iron in the sum of trivalent cations. [b] $\Delta c = \pm0.005$ Å, $\Delta a = \pm0.005$ Å.

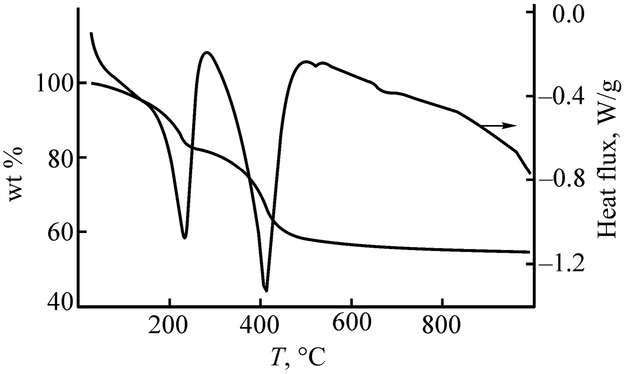

Fig. 2. DSC–TGA curves of the Mg/AlFe$_{10}$ layered hydroxide.

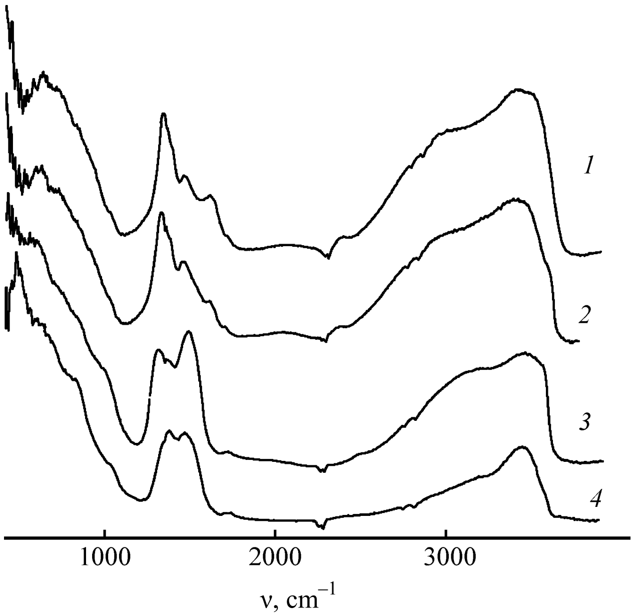

Fig. 3. IR spectra of the Mg/AlFe$_{10}$ hydroxide at (*1*) 25, (*2*) 100, (*3*) 250, and (*4*) 400°C.

O–C–O vibrations of the interlayer carbonate anions, its shoulder at 1635–1655 cm^{-1} being assigned to deformation vibrations of the interlayer water molecules [12].

Analysis of the IR spectra gave additional information on the layered hydroxides structure. The width of the band at 3500 cm^{-1} is usually correlated with ordering of the layered structure: narrower band indicates more uniform ordering of the cations in the layered hydroxide structure [4, 13]. The highest degree of ordering was found in the Mg/AlFe$_6$ and Mg/AlFe$_{11}$ hydroxides and the lowest degree of ordering was observed in the Mg/Fe hydroxide. Those findings coincided with the results of XRD analysis, revealing low crystallinity of the Mg/Fe sample (Fig. 1).

The IR spectra measured at 100°C were similar to those obtained at room temperature; the only difference being weaker bands assigned to deformation of the interlayer water molecules in the cases of some samples. Apparently, heating to 100°C induced partial desorption of the physically bound water, the process being most noticeable in the cases of magnesium- and aluminum-rich samples: Mg/AlFe$_2$, Mg/AlFe$_{11}$, and Mg/AlFe$_{20}$. In the IR spectra measured at 250°C, the bands at 3500–3680 cm^{-1} (assigned to stretching of OH groups in the metal hydroxide layers) were significantly weakened, and the shoulder at 3000 cm^{-1} (assigned to OH stretching of the interlayer water) almost disappeared. The band associated with deformation vibrations of the interlayer water became weaker as well. The observed changes confirmed partial dehydration of all the hydroxides. At 400ºC, the strongest IR bands were those assigned to the M–O vibration region (<800 cm^{-1}), whereas the band at 3600 cm^{-1} almost disappeared.

To conclude, thermal analysis results were in line with those of IR spectroscopy, elucidating temperature range of stability of the layered hydroxides and conditions of their transition into the oxides mixture. In particular, the studied iron-containing hydroxides retained their layered structure up to 200°C and were completely converted into the oxides mixture at 400–450°C.

Study of the texture characteristics of the layered hydroxides revealed a small fraction of micropores (<20 Å in diameter), mesopores (20–500 Å) giving the major contribution to the sample porosity. All the porosity curves contained a peak at 20–30 Å, corresponding to the average interlayer spacing in the metal hydroxides (Table 1). The second maximum was observed at 150–300 Å and likely corresponded to the distance between aggregates (flakes); such aggregates were generally discernible in microscopy images of the hydroxides.

We further studied the so-called “memory effect” of the hydroxides, the ability to restore the layered structure collapsed during calcination. The calcination

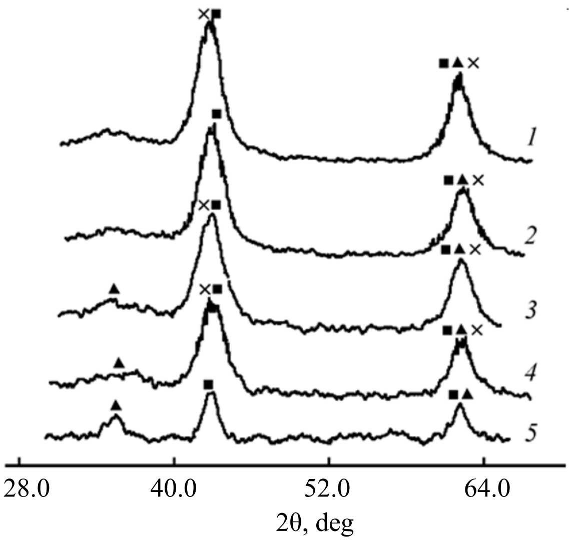

Fig. 4. X-ray diffraction patters of the calcined layered hydroxides: (*1*) $Mg/AlFe_2$, (*2*) $Mg/AlFe_6$, (*3*) $Mg/AlFe_{10}$, (*4*) $Mg/AlFe_{23}$, and (*5*) Mg/Fe. Marks at the peaks show assignment to: (squares) magnesium oxide; (crosses) aluminum oxide, and (triangles) iron oxide.

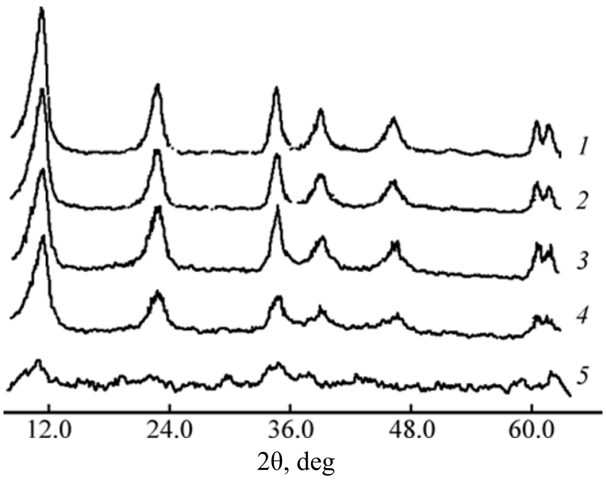

Fig. 5. X-ray diffraction patterns of the rehydrated layered hydroxides: (*1*) $Mg/AlFe_2$, (*2*) $Mg/AlFe_6$, (*3*) $Mg/AlFe_{10}$, (*4*) $Mg/AlFe_{23}$, and (*5*) Mg/Fe.

temperature of 600°C was chosen taking into account the TGA results. XRD patterns of the calcined samples are shown in Fig. 4.

As expected, calcination accompanied with dehydration and dehydroxylation led to disappearance of the layered structure. The XRD patterns of the calcined samples contained reflexes that were definitely assigned to the corresponding metal oxides.

After rehydration, the Mg/Al and $Mg/AlFe_X$ hydroxide samples readily restored their layered structure, as evidenced by the XRD results (Fig. 5). On the contrary, the Mg/Fe hydroxide sample scarcely restored its layered structure after rehydration.

Table 2. Crystal lattice parameters of rehydrated layered hydroxides

Hydroxide	*c*, Å[a]	*a*, Å[a]	*V*, Å^3
Mg/Al	23.49	3.07	191.5
$Mg/AlFe_2$	23.91	3.07	194.7
$Mg/AlFe_6$	23.91	3.07	194.9
$Mg/AlFe_{10}$	24.13	3.07	196.9
$Mg/AlFe_{23}$	23.60	3.07	192.3
$Mg/AlFe_{11}$	23.60	3.08	193.3
$Mg/AlFe_{20}$	23.60	3.07	192.8

[a] $\Delta c = \Delta a = \pm 0.005$ Å.

We calculated the crystal lattice parameters *c* and *a* and crystallite volumes *V* for the rehydrated samples (Table 2).

As seen from the data in Tables 1 and 2, the parameters of the rehydrated samples differed from those of the parent samples. The rehydrated samples were structurally much more similar as compared to the set of initial samples. Apparently, the layered hydroxides formed via dehydration–rehydration were structurally different from the parent samples. Rehydration in an open vessel in air yielded the samples containing carbonate and hydroxide anions; however, the rehydrated samples were likely impoverished with carbonates as compared to the parent samples that were prepared via anion exchange with carbonate. Moreover, the rehydrated samples could be impoverished with iron: in the course of the structure recovery iron could be partially retained in the amorphous phase not registered with the applied methods.

EXPERIMENTAL

Layered hydroxides were synthesized as described elsewhere [14, 15]. The hydroxides were precipitated with NaOH solution from aqueous solution of a mixture of the corresponding metal salts followed by aging under the mother liquor during 2 days at 96–98°C. The next step involved the anion exchange: saturated solution of sodium carbonate was poured onto the precipitate; the mixture was vigorously stirred during 3 h and left for a day; the procedure was then repeated. The excess of sodium salts was removed by washing the product with distilled water until negative sodium test of washings, and the precipitate was dried at 98°C.

X-ray diffraction analysis was performed with the DRON-3 diffractometer (CuK_α radiation, 2θ step of 0.5°). IR spectra were recorded using the Equinox 55 spectrometer in diffuse reflection mode.

The metals content was determined by atomic absorption spectroscopy.

Thermogravimetry and differential scanning calorimetry measurements were performed with the SDT Q600 derivatograph, the sample was heated in air at the rate of 10 deg/min.

The chemical formulas were derived from elemental analysis (cations content and ratio) and thermogravimetry (water content and hydroxide to carbonate ratio) results.

Thermal decomposition was performed in a muffle oven in air at 600°C during 1 h, and then the resulting oxide mixtures were subject to rehydration with distilled water in an open beaker at room temperature during 1 day.

The texture parameters were derived from low-temperature nitrogen adsorption with the Quantachrome AUTOSORB-1C instrument. The samples morphology was visualized with the Quanta 200 3D scanning electron microscope.

The authors are grateful to V.M. Shamshurov† (Shukhov Belgorod State Technological University) for recording the XRD patterns and to S.I. Karpov (Voronezh State University) for registering the IR spectra.

ACKNOWLEDGMENTS

This work was performed in the framework of the Research Project (State Order no.154).

REFERENCES

1. Lebedeva, O., Tichit, D, and Coq, B., *Appl. Catal. A*, 1999, vol. 183, p. 61.
2. Prikhod'ko, R.V., Sychev, M.V., Asterlin, I.M., Erdman, K., Mangel', A., and Van Santen, RA., *Russ. J. Appl. Chem*., 2001, vol. 74, no. 10. p. 1621.
3. Constantino, V.R.L. and Pinnavaia, T.J., *Inorg. Chem*., 1995, no. 34, p. 883.
4. Bellotto, M., Rebours, B., Clause, O., and Lynch, J.A., *J. Phys. Chem*., 1996, vol. 100, no. 20. p. 8527.
5. Vorontsova, O.A., Lebedeva, O.E., and Roessner, F., *Kinet. Catal*., 2009, vol. 50, no. 6, p. 863.
6. Sels, B.F., De Vos, D.E., and Jacobs, P.A., *Catal. Rev*., 2001, vol. 43, no. 4, p. 443.
7. Ryl'tsova, I.G., Vorontsova, O.A., and Lebedeva, O.E., *Butler. Soobshch*., 2011, vol. 27, no. 16, p. 62.
8. Trombetta, M., Ramus, G., Busca, G., Montanari, B., and Vaccari, A., *Langmuir,* 1997, vol. 13, p. 4628.
9. Ryl'tsova, I.G., Matyash, Yu. N., and Lebedeva, O.E., *Sobts. Khromatogr. Prots*., 2010, vol. 10, no. 1, p. 108.
10. Vorontsova, O.A. and Lebedeva, O.E., *Nauch. Ved. BelGU, Ser. Estestv. Nauki*, 2006, no. 3, no. 23, no. 4, p. 24.
11. Vorontsova, O.A., Saenko, R.N., and Lebedeva, O.E., *Russ. J. Inorg. Chem*., 2007, vol. 52., no. 11, p. 1662.
12. Cavani, F., Trifiro, F., and Vaccari, A., *Catal. Today*, 1991, no. 11, p. 173.
13. Eliseev, A.A., Lukashin, A.V., Vertegel, A.A., Tarasov, V.P., and Tret'yakov, V.P., *Dokl. Chem*., 2002, vol. 387, nos. 4–6, p. 339.
14. Vorontsova, O.A. and Lebedeva, O.E., RF Patent no. 2330812, 2008; *Byull. Izobret*., 2008, no. 22.
15. Vorontsova, O.A. and Lebedeva, O.E., RF Patent no. 2361814, 2009; *Byull. Izobret*., 2009, no. 20.